Polarization Rotator on Silicon Strip Waveguide using Tilted Bragg Grating

Eman A. Elzahaby
Dept. of Electron. and Comm. Eng.
E-JUST
Dept. of Eng. Math. and Phys.
Faculty of Eng., Alexandria Uni.
Alexandria, Egypt
eman@alexu.edu.eg

Ahmed M. R. Fath Elbab
Dept. of Mechatron. and Robot.
E-JUST
Alexandria, Egypt
ahmed.rashad@ejust.edu.eg

Hossam M. H. Shalaby
Dept. of Electron. and Comm. Eng.
E-JUST
Dept. of Elect. Eng.
Faculty of Eng., Alexandria Uni.
Alexandria, Egypt
shalaby@ieee.org

***Abstract*—We propose a polarization rotator using partially-etched tilted Bragg grating on a strip waveguide. Our structure features a compact device footprint of 25.2 μm with insertion loss and crosstalk of −1 dB and −20 dB, respectively, while switching the polarization state among fundamental modes (TM/TE).**

***Keywords*—Bragg grating, optical converters, polarization-division multiplexers, polarization rotators, silicon-on-insulator.**

I. Introduction

Recently, devices based on Silicon-on-Insulator platform have gained considerable attention for establishing large-scale photonic integrated circuits (PICs) in optical communications systems, due to its compatibility with complementary metal oxide semiconductor (CMOS) fabrication process, low power consumption and compact footprint [1], [2]. Attributed to the high index contrast between core (Si) and cladding layers (SiO_2) and cross-sectional geometry, the polarization diversity appeared significantly. This property enables upgrading speed and capacity of information transmission and processing by driving advanced multiplexing technology, including polarization-division-multiplexing (PDM), through which dual polarized light are used in a single channel [3]. Another usage for the aforementioned property is to readjust the random polarized light propagating over long distance through optical fibers [4]. That purposes raise the demand of developing devices having the ability to manipulate polarization state such as polarization rotators [5], [6].

In this paper, we design a rotator that switches polarization state among the fundamental modes (TE/TM) propagating in strip waveguide, as a result of partially etched perturbation in the form of tilted Bragg grating. Coupling analysis is addressed to obtain the optimum grating parameters that gain the best performance. Then, the spectral response is determined via 3D-FDTD simulation to verify our device. Unlike other related devices in previous research activities [5], [6], our device combines both compactness footprint and simplicity structure.

II. Characterization

Figure 1 shows our proposed structure which is consisting of a silicon (Si) core layer with thickness $h = 220\,$nm, sandwiched between two silica (SiO_2) layers of thickness $2\,\mu$m, having refractive indices of n_1 and n_2, respectively. That dimensions are in line with standard SOI wafer. A tilted Bragg gratings are engraved on the strip waveguide, having a width of $W = 500\,$nm. According to that width, both TE and TM fundamental modes are supported. That grating has a period of Λ, a depth of d, and a duty cycle of τ, which indicates the percentage between the widths of Si and SiO_2 partitions in a single period, and its plane is tilted in clockwise direction (with respect to y-axis) by an angle θ. That perturbation is extended along a length of $L = N_g\Lambda + W\tan(\theta)$, where N_g is the number of gratings. The ability of exchanging energy from TM_0 into TE_0 can be measured by calculating coupling coefficient as follows,

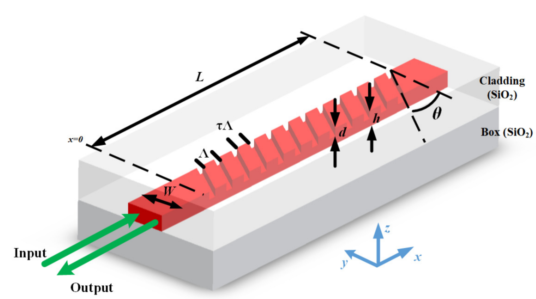

Fig. 1: Perspective view of proposed polarization rotator design.

This work is financially supported by the Ministry of Higher Education, Egypt (MoHE).

$$\kappa^{\mathrm{TM,TE}} = \frac{\pi(n_1^2 - n_2^2)e^{j\pi\tau}\tau\,\mathrm{sinc}\,(\tau)}{\lambda n_{\mathrm{eff}}^{TM}\int_{-\infty}^{\infty}\int_{-\infty}^{\infty}\left([E_x{}^{\mathrm{TM}}(y,z)]^2 + [E_y{}^{\mathrm{TM}}(y,z)]^2 + [E_z{}^{\mathrm{TM}}(y,z)]^2 dydz\right)} \int_{-w/2}^{w/2}\int_{h-d}^{h} e^{+j\frac{2\pi y\tan(\theta)}{\Lambda}}$$
$$\times\left(E_x{}^{\mathrm{TE}}(y,z)[E_x{}^{\mathrm{TM}}(y,z)]^* + E_y{}^{\mathrm{TE}}(y,z)[E_y{}^{\mathrm{TM}}(y,z)]^* + E_z{}^{\mathrm{TE}}(y,z)[E_z{}^{\mathrm{TM}}(y,z)]^* dydz\right), \quad (1)$$

where n_{eff} is the effective index of a propagating mode, λ is the operating wavelength, and E_x, E_y, and E_z are three components of field for each mode. It is should be noticed that grating period is chosen by satisfying phase matched condition to guarantee the feasibility of such coupling using $\Lambda = \lambda/(n_{\mathrm{eff}}^{TM} + n_{\mathrm{eff}}^{TE})$.

III. Numerical Results

First, the effective indices and associated fields of fundamental TE and TM modes are determined using MODE solution at an operating wavelength of 1550 nm, then we calculated the coupling coefficient from (1). In order to find out the optimum grating parameters at which polarization state switches efficiently, we plot the contour of coupling coefficient as function of both grating tilt angle, θ, and duty cycle, τ, at a fixed depth of $d = 70$ nm in Fig. 2. Interestingly, it is obvious that coupling coefficient is a maximum at optimum grating tilt angle of 32°, and that is followed by a local maximum coupling coefficient at grating tilt angle of 62°. That performance refers to a damped sinusoidal term that appears in (1). On the other hand, it is observed that there is a single optimum duty cycle (0.6) at which coupling coefficient is a maximum, that is due to sinc function shown in (1).

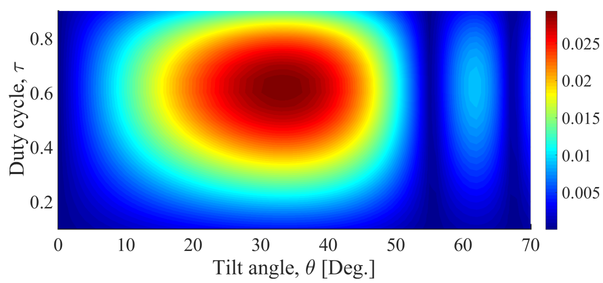

Fig. 2: Contour of coupling coefficient as function of θ and τ.

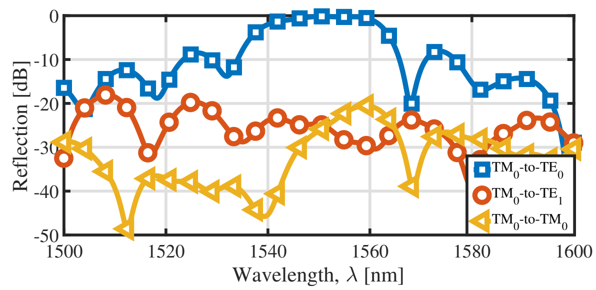

Fig. 3: Simulated wavelength reflection response using 3D-FDTD method.

The proposed rotator is simulated via 3D-FDTD using the aforementioned optimum grating parameters, and its corresponding reflection spectrum response is shown in Fig. 3. In this simulation, a 415 nm corrugation period, 70 nm depth, 0.6 duty cycle, and 32° grating tilt angle are used. A distinct peak is observed at a central wavelength of 1550 nm over a bandwidth of 50 nm from 1535 nm to 1565 nm. The insertion loss of the output mode is −1 dB and maximum crosstalk of the undesired modes is less than −20 dB with a total device length of 25.2 μm. In comparison to what was reported in [5], [6], our converter causes reduction in device's length by ~ 75%. That reduction prevents effect of non-uniformity in the wafer thickness, which adversely affects effective indices when creating long devices [1].

IV. Conclusions

It is concluded that polarization states of fundamental mode rotated efficiently at the presence of tilted Bragg grating partially corrugated on a strip silicon waveguide. After choosing the optimum grating parameters from coupling coefficient calculations, the rotator has been executed with insertion lose of −1 dB and compact length of 25.2 μm. Our device has a privileged of compactness and simplicity compared to other previous related reported devices.

References

[1] W. Bogaerts, and L. Chrostowski, "Silicon Photonics Circuit Design: Methods, Tools and Challenges," Laser Photonics Reviews, vol. 12, pp. 1950–1955, June 2018.
[2] A. Mistry, M. Hammood, S. Lin, L. Chrostowski and N. A. F. Jaeger, "Effect of lithography on SOI, grating-based devices for sensor and telecommunications applications," 2019 IEEE 10th Annual Information Technology, Electronics and Mobile Communication Conference (IEMCON), 2019, pp. 0932-0938.
[3] C. Li, D. Liu, and D. Dai, "Multimode silicon photonics," Nanophotonics, vol. 8, pp. 227–247, June 2019.
[4] T. Koonen, "Fiber to the Home/Fiber to the Premises: What, Where, and When?," in Proceedings of the IEEE, vol. 94, no. 5, pp. 911-934, May 2006.
[5] H. Okayama, Y. Onawa, D. Shimura, H. Yaegashi, and Hironori Sasaki, "Polarization rotation Bragg grating using Si wire waveguide with non-vertical sidewall," Opt. Express, vol. 22, pp. 31371–31378, December 2014.
[6] H. Okayama, Y. Onawa, D. Shimura and H. Yaegashi, and Hironori Sasaki, "Polarization rotation Bragg grating using Si waveguide with top surface groove grating and terrace," Japanese Journal of Applied Physics, vol. 57, pp. 042201(1-7), February 2018.